Best practices for ORR performance evaluation of metal-free porous carbon electrocatalysts

L. Bouleau, Sara Pérez-Rodríguez, Javier Quilez-Bermejo, M.T. Izquierdo, Feina Xu, Vanessa Fierro, Alain Celzard

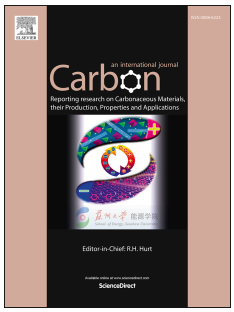

Best practices for ORR performance evaluation of metal-free porous carbon electrocatalysts

L. Bouleau, S. Pérez-Rodríguez, J. Quílez-Bermejo, M.T. Izquierdo, F. Xu, V. Fierro, A. Celzard

PII: S0008-6223(21)01237-9

DOI: https://doi.org/10.1016/j.carbon.2021.12.078

Reference: CARBON 16902

To appear in: *Carbon*

Received Date: 29 August 2021

Revised Date: 17 December 2021

Accepted Date: 22 December 2021

Please cite this article as: L. Bouleau, S. Pérez-Rodríguez, J. Quílez-Bermejo, M.T. Izquierdo, F. Xu, V. Fierro, A. Celzard, Best practices for ORR performance evaluation of metal-free porous carbon electrocatalysts, *Carbon* (2022), doi: https://doi.org/10.1016/j.carbon.2021.12.078.

Credit Author Statement

LB made the first experiments and contributed to writing the original draft. SPR and JQB completed the experiments with many new data and worked on the draft. All other authors contributed equally to the writing and editing of the final version.

Graphical abstract

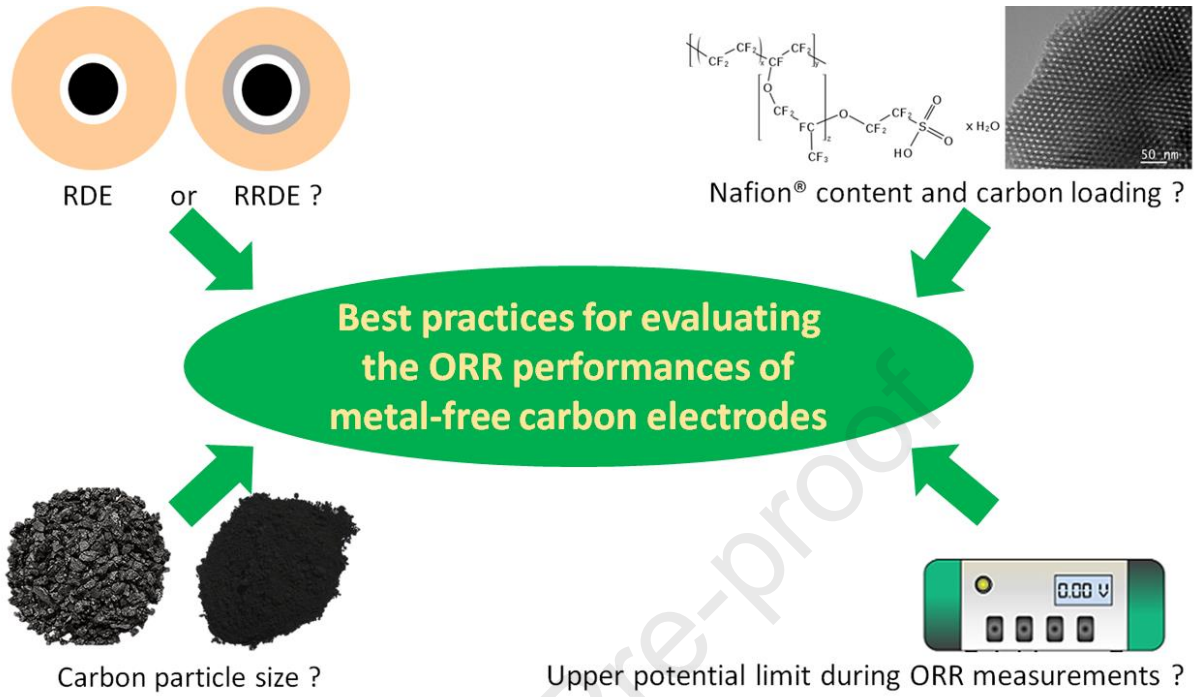

Best practices for ORR performance evaluation of metal-free porous carbon electrocatalysts

L. Bouleau[1,2], S. Pérez-Rodríguez[1], J. Quílez-Bermejo[1], M.T. Izquierdo[3], F. Xu[2], V. Fierro[1], A. Celzard[1*]

[1] Université de Lorraine, CNRS, IJL, F-88000 Epinal, France

[2] Université de Lorraine, CNRS, LEMTA, F-54000 Nancy, France

[3] Instituto de Carboquímica (ICB-CSIC), Miguel Luesma Castán 4, E-50018, Zaragoza, Spain

[*] Corresponding author. Tel: + 33 372 74 96 14. E-mail address: alain.celzard@univ-lorraine.fr (A. Celzard)

Abstract

Porous carbon materials are promising electrocatalysts for the oxygen reduction reaction (ORR). Their active sites, involving porosity and surface chemistry, are different from those of metal-doped carbons. The latter have been widely studied and are adapted to today's popular electrochemical devices, the rotating disk electrode being the most useful preliminary tool to evaluate their activity in ORR. However, porous carbon materials have been less explored, and experimental parameters need to be adjusted to achieve the best ORR performance. Therefore, in this study, the optimization of different key factors was investigated to evaluate their effect on the ORR performance of porous carbon electrocatalysts in alkaline medium. The parameters considered were: (i) the relevance of using RRDE or Koutecky-Levich equations for estimating the number of electrons transferred; (ii) the amount of ionomer (Nafion®); (iii) the carbon loading on the electrode; (iv) the carbon grinding method; and (v) the selection of the upper potential of ORR experiments. We conclude that an optimization of the experimental conditions should be done for each material studied, and we give important benchmarks for the appropriate evaluation of the catalytic activity in ORR of carbon-based catalysts.

Keywords: Oxygen reduction reaction; Porous carbons; Fuel cells; Electrocatalysts.

1. Introduction

The development of new metal-free catalysts for the oxygen reduction reaction (ORR) is an extremely active research topic nowadays. This subject is particularly challenging for the development of fuel cells and metal-air batteries [1–6]. The ORR is a very complex electrochemical reaction that involves multiple steps. In brief, the reduction of the dioxygen molecule may occur through two main general mechanisms in an aqueous electrolyte: (i) by the 4-electron pathway, in which the oxygen molecule is reduced directly into two water molecules (or 4 OH^- in alkaline medium); and ii) by the 2-electron pathway to produce one hydrogen peroxide molecule (or OOH^- in alkaline medium). This hydrogen peroxide (or OOH^-) can be further reduced into two water molecules (or 4 OH^-), thus completing a 2+2 electron pathway. As a result, the number of electrons transferred during ORR can theoretically be two (2-electron pathway) or four (4- or (2+2)-electron pathways), depending on the nature and number of active sites of the electrocatalysts. In catalysts with multiple active sites, the combination of all these mechanisms may lead to a number of electrons transferred between 2 and 4.

The most common ORR electrocatalyst consists of platinum-group metal nanoparticles deposited onto carbon materials [7], although electrodes based on non-precious transition metals (*e.g.*, Fe [8], Co [9] or Mn [10]) have also been proposed as alternative catalysts. However, platinum has several drawbacks such as high cost and low availability, and the other possible metals suffer from poor durability, especially under acidic conditions. Over the past decade, many efforts have been made to develop metal-free carbon catalysts for ORR. Activity similar to the state-of-the-art Pt-based electrocatalyst and long-term stability have been achieved by some carbon materials doped with different heteroatoms (such as N, B, S or P) [1,5,11].

Despite these promising results, there is still a lack of research in testing protocols for metal-free carbon electrodes. Indeed, the literature on this topic is very confusing, and authors do not

agree on how to make measurements, which can make published results very difficult to compare with each other. In general, the activity for the ORR is studied after casting a thin layer of electrocatalyst onto a rotating disk electrode (RDE) or a rotating ring disk electrode (RRDE) in half-cell configurations. Whereas standardization of experimental methods to quantify the activity of Pt/C and carbon-supported noble-metal catalysts for ORR has been extensively studied [12–18], analytical procedures for accurate comparison of metal-free porous carbon electrocatalysts have been rarely reported [19–23]. Additionally, the influence of experimental conditions on ORR performance has been even less explored (*e.g.* carbon loading, binder amount, carbon particle size, and working electrode preparation and composition) [19–23]. From our own experience, the choice of experimental conditions has an enormous influence on the catalytic results. Consequently, very different performances can be obtained depending on these operating factors. This is extremely confusing and does not help newcomers to identify the key parameters that need to be optimized. On the other hand, most of the work devoted to the activity of metal-free carbon electrodes for ORR focus on the introduction of different heteroatom moieties and the textural properties are not considered in detail. However, porosity plays a key role on the electrochemical activity for ORR, being decisive for metal-free carbon-based catalysts [24–26], and a thorough analysis should be carried out for these particular materials.

In this work, we investigate the influence of relevant operating parameters that affect the performance of electrocatalysts based on porous carbon materials for ORR. These are the relevance of using the rotating ring-disk electrode (RRDE) or the Koutecky-Levich (KL) equations for estimating the number of electrons transferred, the amount of ionomer (Nafion®), the carbon loading on the electrode, the carbon grinding method, and the selection of the upper potential during ORR measurements. The results provide important information for best practices and evaluation of ORR performance of metal-free porous carbon materials.

2. Experimental

2.1 Materials

Two porous carbon materials (CM) were selected for this study: one with moderate porosity (P-CM) and one with a much higher porosity (HP-CM). Additionally, two commercial carbon materials were also used for comparison purposes: C30X (also known as MSC30), supplied by Kansai Coke and Chemicals Co., and CW30, supplied by Silcarbon & Aktivkohle.

The P-CM sample was prepared by mechanosynthesis of condensed (mimosa) tannin with Pluronic® F127 and water in a mass ratio of 1:1:1. More details about the synthesis and the corresponding physicochemical characterization can be found elsewhere [27]. For the mechanosynthesis, a PM 100 planetary ball milling system (Retsch) was used at 500 rpm with 10 agate balls of 10 mm of diameter for 1 h in an agate bowl. After the ball milling process, a paste-like material was recovered, which was heat-treated at 900 ºC in a tubular furnace for 1 h under a nitrogen flow of 100 $mL \cdot min^{-1}$. The resulting carbon was named P-CM.

HP-CM was obtained by increasing the porosity of P-CM by physical activation. P-CM was heated up to 900 °C (5 °C min^{-1}) under a stream of nitrogen (100 mL min^{-1}), then the stream was changed to CO_2 (50 $mL \cdot min^{-1}$) for 45 min before returning to nitrogen for cooling. After CO_2 activation, the material was heat-treated at high temperature (1500 ºC, 1 $ºC \cdot min^{-1}$, 200 $mL \cdot min^{-1}$ Ar flow) to ensure proper removal of oxygen groups created during physical activation. The resultant material was designated HP-CM.

Two different methods were then used to reduce the size of the as-obtained particles of porous carbon: (i) hand-grinding in an agate mortar for 15 min; or (ii) vibrational ball milling using a Mixer Mill MM 400 (Retsch), equipped with a 1.5 mL grinding jar and two 5 mm diameter steel balls, and operated at a frequency of 25 Hz for 10 min. It should be pointed out

here that no iron impurities from the steel balls were introduced by vibrational milling, as confirmed by the Fe2p spectra for the HP-CM and P-CM samples in Figure S1.

2.2 Physicochemical characterization

The particle size distribution of the carbon materials was determined by laser diffraction using a Mastersizer 3000 (Malvern Panalytical) analyzer. Prior to the analysis, the carbon powders were dispersed in ethanol.

N_2 adsorption-desorption isotherms were measured at -196 °C with a Micromeritics ASAP 2020 automatic adsorption system. Prior to adsorption measurements, the samples were outgassed at 150 °C for 12 h under vacuum. The BET area (A_{BET}, $m^2\ g^{-1}$) was obtained by applying the well-known Brunauer-Emmett-Teller method. CO_2 adsorption isotherms were obtained at 0 °C with a Micromeritics ASAP 2040 automatic adsorption device. Specific surface areas (S_{NLDFT}, $m^2\ g^{-1}$), total pore volumes (V_T, $cm^3\ g^{-1}$) and micropore volumes (V_μ, $cm^3\ g^{-1}$) were obtained by applying the 2D non-local density functional theory for heterogeneous surfaces (2D-NLDFT-HS) to both N_2 and CO_2 adsorption isotherms. Micromeritics SAIEUS® software was used for data processing by applying the 2D-NLDFT-HS method.

X-ray photoelectron spectroscopy (XPS) spectra were obtained with an ESCAPlus OMICROM spectrometer equipped with a non-monochromatized Mg Kα X-ray source. Survey scans and C1s and O1s high-resolution scans were recorded at 10 kV and 15 mA using analyzer pass energies of 50 and 20 eV, respectively. Binding energies were referenced to the C1s peak (284.5 eV). Shirley-type background subtraction, peak fitting and quantification were processed by CASA software.

Raman spectra were recorded with a Horiba XploRa Raman apparatus equipped with a 50× long-range objective. The spectra were obtained using a holographic grating with 1200 lines per mm and circularly polarized lasers (wavelengths of 532 and 638 nm, both filtered at 10%

of their maximum energy to avoid heating of the samples) in the Raman shift range of 200 to 3800 cm^{-1}. The spectra obtained at a wavelength of 638 nm was then treated by the method described by Mallet-Ladeira et al. [28], using a double Lorentzian for the D band and an asymmetric mixed Gaussian-Lorentzian profile for the G band with Labspec6 software (Horiba). The crystallite size L_a (nm) was then deduced from the half width at half maximum of the G band, $HWHM_G$ (cm^{-1}), according to Eq. (1) [28]:

$$HWHM_G = (68 \pm 4) - (5.2 \pm 0.5)\, L_a \quad (1)$$

which is valid for L_a below ~ 10 nm, a situation that is obviously applicable to the activated carbons discussed here.

2.3 Electrochemical characterization

The electrochemical characterization of P-CM and HP-CM was carried out in a traditional three-electrode cell with a speed rotor and a rotating ring-disk electrode (RRDE) connected to a PGSTAT302N bi-potentiostat (Metrohm). The working electrode consisted of a glassy carbon disk (0.196 cm^2) and a platinum ring as a second working electrode. The electrode reference was a silver/silver chloride (Ag / AgCl / 3M KCl), although all potentials were referred to the reversible hydrogen electrode (RHE) when discussing the results. In addition, a glassy carbon rod (8 mm diameter) was used as the counter electrode. Electrochemical measurements were performed in alkaline medium (0.1 M KOH, pH = 13) at 20 °C. Unless otherwise specified, P-CM and HP-CM powders were suspended (1 mg mL^{-1}) in an isopropanol/water (20/80, v/v) solution, to which 5 µL of Nafion® dispersion (5 wt.%, Sigma-Aldrich) was added under sonication. 6 aliquots of 8.18 µL of the resulting ink were drop-cast onto the glassy carbon disk until a carbon loading of 0.25 mg·cm^{-2} was reached. The carbon/Nafion® mass ratio of the catalyst thin layer was of 4.6 (corresponding to a Nafion® weight ratio of 17.9%). Different Nafion® contents and carbon loadings were also tested.

Prior to the ORR measurements, the RRDE electrode was immersed in the working solution under vacuum to ensure optimal wettability. Then, the electrode was immersed in the electrolyte for 25 min under continuous nitrogen bubbling. Cyclic voltammetry (CV) scans from 1 to 0 V vs. RHE were recorded at different scan rates: 50 mV s^{-1} (20 cycles), to stabilize the electrode in the window potential range in which ORR takes place, and 5 mV s^{-1} (2 cycles), to evaluate the double-layer current. After that, the working solution was saturated with oxygen under continuous flow for 25 min. Then, linear sweep voltammetry (LSV) measurements were carried out at different rotation rates (400 – 2025 rpm) with a scan rate of 5 mV s^{-1} under continuous oxygen flow from the upper potential limit (in a conventional test: 1 V vs. RHE) to 0 V vs. RHE. All the LSV curves presented in this paper, unless otherwise specified, are those obtained at 1600 rpm and were corrected by subtracting the double-layer current measured during the CV test under N_2-saturated solution at a scan rate of 5 mV s^{-1} [14,21]. In addition, the currents were always normalized by the geometrical area of the disk (0.196 cm^{-2}). During the ORR measurements, the platinum ring potential was fixed at 1.5 V vs. RHE, to ensure oxidation of any hydrogen peroxide generated by the catalyst.

The overall electron transfer number (n) was calculated from the currents of the working electrode and the platinum ring measured during the LSV experiments at 1600 rpm according to Eq. (2):

$$n = \frac{4\, I_D}{I_D - \frac{I_R}{N}} \qquad (2)$$

where the ring current and the disk current are denoted I_R (A) and I_D (A), respectively, and N is the collection efficiency of the RRDE. N was determined experimentally by the reversible redox couple $[Fe(CN)_6]^{3-/4-}$ using the bare glassy carbon (GC) disk [29]. I_D and I_R were recorded in the presence of 0.1 M KOH and 0.01 M $K_3Fe(CN)_6$ at 5 mV s^{-1} and at different rotation rates. The platinum ring was fixed at 1.5 V vs. RHE. Figure S2 shows that the ring current density is

controlled by mass transfer and thus the collection efficiency can be obtained by the I_R/I_D ratio. A constant N of 0.265 was found at the different rotation rates (Figure S2c).

The percentage of hydrogen peroxide produced (H_2O_2 %) can also be evaluated from the same parameters, using Eq. (3):

$$H_2O_2\% = 200 \cdot \frac{\frac{I_r}{N}}{I_D + \frac{I_R}{N}} \quad (3)$$

The onset potential, E_{ONSET} (V), was measured at a current density of -0.1 mA·cm^{-2} for all samples consistent with previous works [21,30,31].

3. Results and discussion

3.1 Rotating ring-disk electrode vs. Koutecky-Levich equations

Historically, the electron number for the ORR was determined by application of the Koutecky-Levich equation using an RDE. Nowadays, the development of RRDE allows for better interpretation of the data since the percentage of hydrogen peroxide generated during ORR can be measured experimentally by a second working electrode. To illustrate the difference between these methods and their application in evaluating the performance for ORR of carbon-based electrocatalysts, a carbon material with moderate porosity (P-CM) and a highly porous carbon material (HP-CM) were analyzed by RDE and RRDE. The main textural parameters of these carbon materials are summarized in Table 1, as well as those of commercial activated carbons used for comparison purposes in this paper.

Table 1. Textural parameters of lab-made (P-CM and HP-CM) and commercial (C30X and CW30) porous carbon materials.

Sample	A_{BET} [a] ($m^2\ g^{-1}$)	S_{NLDFT} [b] ($m^2\ g^{-1}$)	V_T [c] ($cm^3\ g^{-1}$)	V_μ [d] ($cm^3\ g^{-1}$)

P-CM (as-synthesized)	550	850	0.49	0.22
HP-CM (as-synthesized)	1270	1170	0.96	0.42
HP-CM (after ball milling)	1350	1450	1.04	0.48
C30X (as-received)	3200	2500	1.64	0.98
C30X (after ball milling)	3080	2130	1.45	0.90
CW30 (as-received)	1735	1520	1.46	0.58
CW30 (after ball milling)	1645	1375	1.20	0.53

[a] A_{BET}: Brunauer–Emmet–Teller (BET) area; [b] S_{NLDFT}: specific surface area obtained by application of the 2D non-local density functional theory model for heterogeneous surface (2D-NLDFT-HS); [c] V_T: total pore volume derived from the 2D-NLDFT-HS; [d] V_μ: micropore volume derived from the 2D-NLDFT-HS.

In a common RRDE test, a constant potential is applied to the platinum ring (typically 1.2 – 1.6 V vs. RHE), which is high enough to oxidize the hydrogen peroxide formed during oxygen reduction on the disk but prevents the evolution of oxygen from water. A collection efficiency ratio, *N*, must be taken into account to evaluate the actual percentage of H_2O_2 travelling from the disk to the ring. The number of electrons transferred, *n*, and H_2O_2 formation are calculated with Eq. (2) and (3), respectively.

On the other hand, the commonly used methodology for determining the transfer electron number for the ORR without RRDE equipment is based on the Koutecky-Levich (KL) equation:

$$\frac{1}{j} = \frac{1}{j_d} + \frac{1}{j_k} = \frac{1}{B\omega^{1/2}} + \frac{1}{j_k} \quad (4)$$

where j, j_d and j_k represent the global current density, diffusion-limited current density and kinetic current density, respectively. The current densities are obtained by normalizing the currents by the geometric area of the electrode (cm^2). ω (rad s^{-1}) is the rotation speed of the electrode, and B is the Levich constant, expressed as follows:

$$B = (0.62)\, n\, F\, D^{2/3}\, v^{-1/6}\, C \quad (5)$$

with n being again the number of electrons transferred, F the Faraday constant (C mol^{-1}), D the diffusion coefficient of oxygen in the electrolyte (cm^2 s^{-1}), ν the kinematic viscosity of the electrolyte (cm^2 s^{-1}) and C the analyte concentration (mol cm^{-3}).

By measuring the current at different rotation speeds and applying Eq. (4), *i.e.*, by plotting -1/j as a function of $\omega^{-1/2}$, it is possible to evaluate the number of electrons transferred at different potentials.

The LSV curves of the materials, shown in Figure 1a, revealed two waves for the ORR attributed to a 2+2 electrons pathway. At a potential range of 0.6 – 0.4 V vs. RHE (medium overpotentials), the first current plateau appears with an electron transfer close to 2.0 – 2.5 (depending on the carbon and the rotation speed), due to the formation of H_2O_2. In contrast, at potentials below 0.4 V, H_2O_2 is further reduced to H_2O and a second plateau is observed at ≈ 0 V with n values around 3.0 – 3.3. It is worth mentioning that hydrogen-powered fuel cells operate at an average single-cell voltage within the range 0.8 – 0.6 V, whereas the typical voltage for direct methanol fuel cells is about 0.5 – 0.35 V. Therefore, the electron transfer number at the first plateau is more realist from an operation point of view, whereas the values at 0.0 V evidence the 2+2 reaction mechanism.

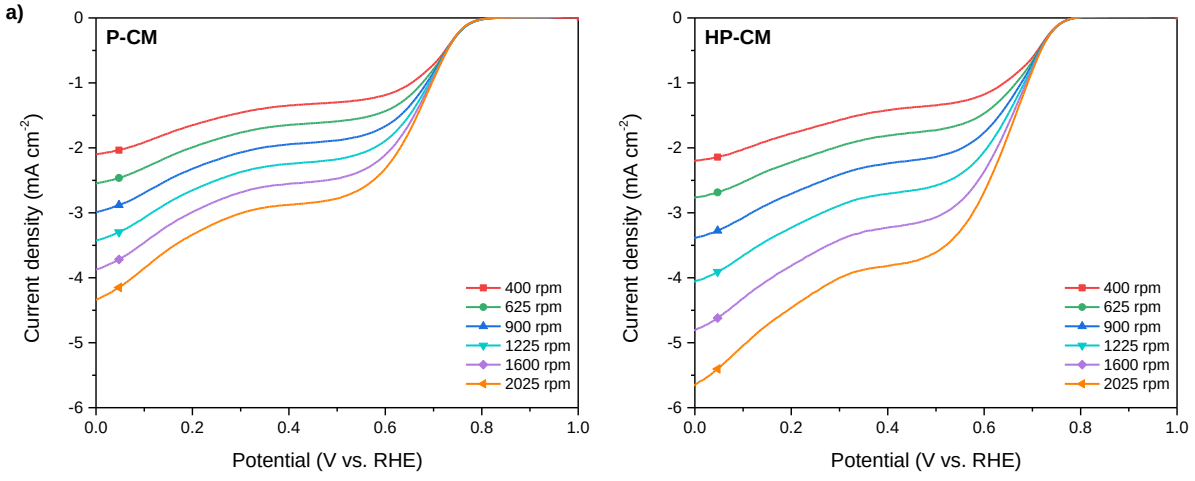

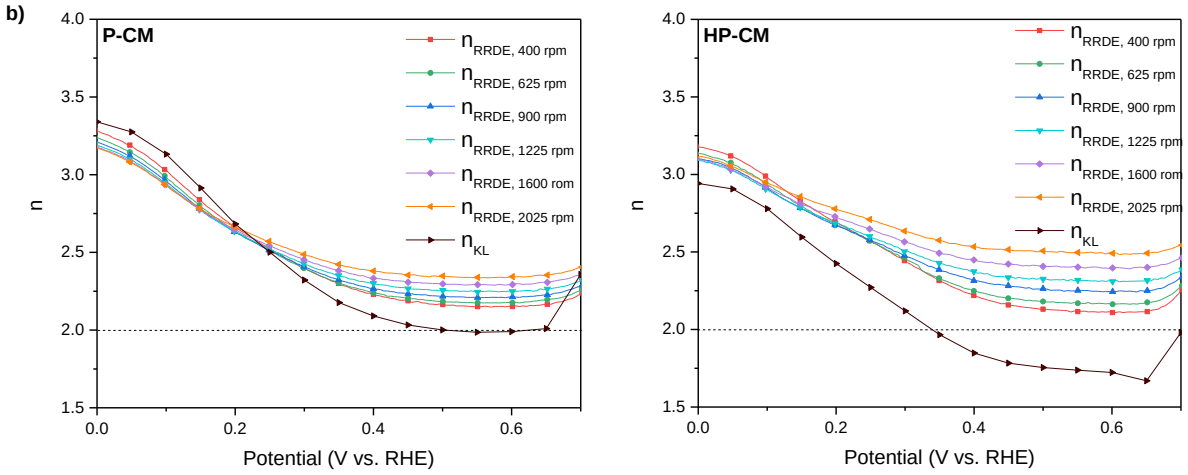

Figure 1. (a) LSV curves and (b) number of electrons transferred (*n*) for ORR measurements with P-CM and HP-CM. *n* was calculated either from RRDE at different rotation rates, from 400 to 2025 rpm, or from the Koutecky-Levich equation, in 0.1 M KOH solution saturated with O_2. The other conditions were: scan rate 5 mV s^{-1}; 17.9 wt.% Nafion®; carbon loading 0.25 mg cm^{-2}. Prior to the electrochemical measurements, the materials were ball-milled (see Section 3.2).

Comparing the current density (mA cm^{-2}) at the same rotation speed, a higher ORR activity for HP-CM than for P-CM was observed. This is directly ascribed to the larger surface area of the former material, which provides a higher amount of active sites for the ORR. Additionally, the RRDE results showed that ω plays an important role on the electron transfer number: the faster the rotation speed, the higher the electron transfer in the potential range of 0.7 – 0.2 V vs. RHE (*i.e.*, the selectivity towards hydroxide increases). This could be related to a higher flux of electroactive species to the electrode surface by increasing ω (convection), and thus lead to the possibility for oxygen to access more catalytic sites (micropores) to form H_2O_2 (2 electron-pathway). Subsequently, the H_2O_2 produced can be adsorbed in these micropores, promoting further reduction to hydroxide, and thus leading to higher values of *n* at medium potentials (2+2 electron-pathway) [19]. In line with this assumption, a greater increase in the number of electrons transferred with rotation rate was observed for the highly porous carbon material with

a larger amount of micropores, HP-CM (V_μ = 0.48 cm^3 g^{-1}, see Table 1), which increases the contact time with H_2O_2, and thus the rate of hydrogen peroxide conversion. Experiments on the calibration of the collection efficiency (N) at different rotation rates by the $[Fe(CN)_6]^{3-/4-}$ redox reaction at an RRDE electrode loaded with the HP-CM catalyst (0.25 mg cm^{-2}) were performed to rule out inaccuracies in the calculated number of electrons transferred due to turbulence in the electrolyte flow, possibly induced by a rough carbon coverage [15]. Nearly identical N values were obtained for the unloaded and loaded electrodes (Figure S2c). Additionally, hydrodynamic experiments of the loaded electrode also showed a constant collection efficiency over the range of rotation rates, as previously reported by other authors for low carbon loadings [15]. Therefore, the increase in the number of exchanged electrons as ω increases in the potential window from 0.7 to 0.2 V vs. RHE cannot be explained by deviations in collection efficiency by turbulence issues. On the other hand, at less positive potentials (from 0.2 to 0.0 V vs. RHE), the electron transfer does not depend on the rotation rate (or n even decreases at higher ω). Therefore, the higher selectivity towards hydroxide at high overpotentials seems to be related to the internal diffusion rates of both O_2 and H_2O_2 in restricted catalytic sites (narrow micropores), which is not related to ω, as previously proposed Gabe et al. [19].

The above results show that the assumption that n is not influenced by the rotation speed, necessarily made to apply the KL equation, is not valid for these carbon materials, in particular in the potential range from 0.7 to 0.2 V vs. RHE. The number of electrons transferred calculated by the two methods, KL (n_{KL}, Eq. (4) and (5)) and RRDE (n_{RRDE}, Eq. (2)), are shown in Figure 1b for P-CM and HP-CM. n_{KL} and n_{RRDE} are slightly different for P-CM. However, substantial discrepancies in the electron number estimated by both methods were found for the carbon with the most developed porosity (HP-CM), with n_{RRDE} values being higher than those determined by KL throughout the potential window. KL is a theory developed for first-order reversible reactions, based on the normalization of current densities by the geometric area of the working

electrode and, consequently, the quantification of the diffusion-limited current density or the electron number depends on the substrate area. Working electrodes for ORR testing are usually prepared by depositing a thin layer of material on the substrate by drop casting. When a flat and smooth electrode is used, the entire area exposed to the electrolyte is the same as the geometric area. However, in porous materials such as carbon-based electrocatalysts, the area that can interact with dioxygen molecules (including inner porosity) is significantly larger than the geometric area, and this is not accounted by the KL equations. Moreover, such microporosity can increase the retention time of the ORR by-products, leading to a second reduction process within the porous structure of the carbon material [19]. Therefore, the use of the KL equation in porous carbons is not adequate if accurate results are needed.

This effect is higher for the sample HP-CM, in which the BET area is around 1350 $m^2\ g^{-1}$ after ball milling. The difference between the KL and RRDE results is larger, underestimating the number of electrons when the KL equations are used. Indeed, the number of electrons transferred during ORR measurements are lower than 2 at potentials above 0.3 V vs. RHE, which is theoretically impossible since dioxygen molecules cannot be reduced by less than 2 electrons. The KL method assumes that the diffusion-limited current density (j_d) is a direct function of $\omega^{1/2}$ and that the number of electrons transferred does not depend on ω (see Eq. (4) and (5)). However, the RRDE experiments demonstrate that this statement is false since n depends on the rotation speed: n increases with ω from 0.7 to 0.2 V for both carbon materials (especially for HP-CM). This higher value of n leads to a faster increase in j_d than assumed by the KL method (based on Eq. (4)), and hence, the KL slope (denoted by B in Eq. (4) and (5)) is overestimated (*i.e.*, is higher than it should be). The higher KL slope results in lower calculated values of n_{KL} (even exhibiting lower values for HP-CM than the theoretical minimum number of electrons transferred) [15]. Therefore, the higher rate of oxygen reduction at the carbon electrode through increased convection (higher ω) and the presence of micropores promote

H_2O_2 adsorption and, consequently, lead to additional reduction to hydroxide and higher values of *n* at medium potentials as determined by RRDE experiments (see Figure 1b). This increase in electron transfer results in an underestimation of n_{KL}. In the potential range of 0.2 to 0.0 V vs. RHE, *n* is independent of ω (or slightly dependent), and the electron numbers determined by the RRDE and KL equations are more similar. However, the values of n_{KL} and n_{RRDE} still differ due to discrepancies between geometric surface area and effective electrochemical area of carbon.

This behavior is not only specific to these lab-made porous carbons. Indeed, LSV and *n*-potential curves at several ω for a commercial activated carbon (C30X) with a highly developed porosity (A_{BET} of 3080 m^2 g^{-1} after milling) also show an increase in the number of electrons transferred with rotation rate at medium overpotentials, and exhibit n_{KL} values below 2 in the potential range 0.7-0.4 V vs. RHE (see Figure S3). Furthermore, Zhou et al. recently reported similar results for a typical carbon-based electrocatalyst: electrochemically reduced graphene oxide [15]. Comparing the LSV and electron transfer-potential curves at 1600 rpm of the lab-made porous carbon materials (P-CM and HP-CM) and the commercial sample (C30X) (Figure S4), a clear influence of textural properties on the ORR activity is noted. More developed surface area and microporosity led to higher current density and selectivity for hydroxide, with C30X being the most active material for oxygen reduction. Besides a developed surface area, other parameters such as the micro-mesopore ratio, pore size, carbon structure, surface chemistry, etc., also play an important role. This is evident in Figure S4, where CW30, another commercial sample with an A_{BET} about 3 and 1.2 times higher than those of P-CM and HP-CM showed substantially lower activity for ORR.

In summary, the dependence of *n* on the rotation rate invalidates the KL theory for drop-cast electrodes and reinforces the need for highly accurate equipment, such as RRDE, to characterize porous carbon materials for electrochemical reactions. Furthermore, as demonstrated by P-CM

and HP-CM, the higher the specific surface area of the porous carbon, the greater the need to use RRDE. This seems to be related to the importance of microporosity in the ORR performance. Micropores induce the retention of ORR by-products, and hence, condition the activity for the reduction of both O_2 and H_2O_2 [19]. This increase in the residence time of hydrogen peroxide is expected to be greater as the surface area and micropore volume increase. The results obtained by the KL method should only be applied in specific cases, such as a homogeneous flat surface and/or a low surface area. Nevertheless, if possible, it is always advisable to work with an RRDE system to avoid most of these problems when evaluating the performance of carbonaceous materials.

In the following sections of this paper, we will only show the transferred electron values obtained by the RRDE technique in order to provide an accurate discussion of the relevance of the different experimental parameters on the ORR. Moreover, since HP-CM is the material with a higher activity for ORR due to its larger surface area, we have selected this sample for the next experiments.

3.2 Effect of grinding the carbon material

The lab-made HP-CM material presents an average particle size too large to expose properly the active sites. Therefore, it can be expected that grinding would be required to decrease the particle size and improve the electrocatalytic activity for ORR. This material was ground using two approaches: (i) vibrational ball milling for 10 min; and (ii) manual grinding in an agate mortar for 30 min. This section addresses the electrocatalytic performance for oxygen reduction of the as-synthesized material and the carbon powder obtained using the different grinding methods. First, the influence of milling on the particle size but also on the carbon structure, surface chemistry and textural properties is evaluated.

3.2.1 Physicochemical characteristics

The particle size distributions of HP-CM and its milled counterparts are given in Figure 2a. The pristine material presents a broad unimodal distribution centered around 330 µm. Upon ball milling or mortar grinding, the particle size was significantly reduced to 60 and 35 µm, respectively. However, a fraction of the particle population larger than 400 µm was also observed when the sample was subjected to mortar grinding. Therefore, ball milling appears to be a more effective treatment to homogeneously decrease the particle size.

In addition to the decrease in particle size, grinding may induce the generation of defects in the carbon structure and the decrease in crystallite size, as deduced from the Raman spectra of HP-CM before and after ball milling. Figures S5a and S5b show in particular that, whatever the wavelength of the used laser, the intensity ratio of the D/G bands decreased after milling: from 1.77 to 1.48 at 532 nm, and from 1.93 to 1.69 at 638 nm. As HP-CM is a non-graphitizable carbon, this evolution is consistent with the creation of structural defects, also known as stage 2 of the amorphization trajectory of carbons [32]. This finding is corroborated by a broadening of the G band whose half width at half maximum, obtained after fitting the Raman profile (see Figure S5c), increased from 47 to 51 cm^{-1}. Although modest, this broadening allows us to calculate from Eq. (1) a significant decrease in the average value of L_a, from 4.0 (± 1.2) nm before milling to 3.3 (± 1.1) nm after milling. This decrease in crystallite size is also in agreement with the slight change in the position of the G band, whose Raman shift is expected to increase [33], here from 1603 cm^{-1} before milling to 1608 cm^{-1} after milling. In the same way, and even if this effect is generally much less marked, it has been observed for graphitizable or non-graphitizable carbons that the D band moves, from a minimal position obtained with a L_a of the order of 4 nm, towards greater Raman shifts when L_a decreases below 4 nm [33]. This is indeed what is observed here, with a D band centered at 1317 cm^{-1} before milling ($L_a \sim 4$ nm) and at 1324 cm^{-1} after milling ($L_a < 4$ nm).

The surface composition and chemistry of the as-synthesized material and its milled counterpart was studied by XPS (see Figure S6 and Table S1). The pristine HP-CM exhibits low surface oxygen content (~ 2 at. %, see Table S1), which is attributed to the removal of oxygen-containing species (generated by CO_2 activation) during heat treatment at 1500 °C. Both grinding methodologies resulted in a slight increase in oxygen moieties (not exceeding 1 at. % over the non-ground material) through fragmentation of carbon particles in the presence of air. Grinding also had no substantial influence either on oxygen speciation, as can be better seen in the high-resolution C1s and O1s spectra given in Figure S6. The grinding methods led to a slight removal of anhydride groups (as shown by the decrease in CII and OII contributions, see again Table S1) and an increase in the density of quinones and carbonyls (as shown by the increase in CIII and OI in Table S1).

Data obtained from N_2 and CO_2 adsorption isotherms (Table 1) show the changes in textural properties after ball milling of pristine HP-CM. These results show a moderate increase in A_{BET}, from 1270 to 1350 $m^2\ g^{-1}$, and S_{NLDFT}, from 1170 to 1450 $m^2\ g^{-1}$ after ball milling. A slight increase in total pore volume and micropore volume is also detected after such grinding.

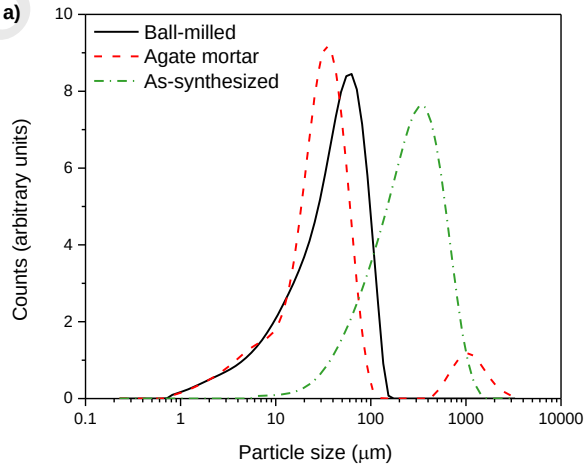

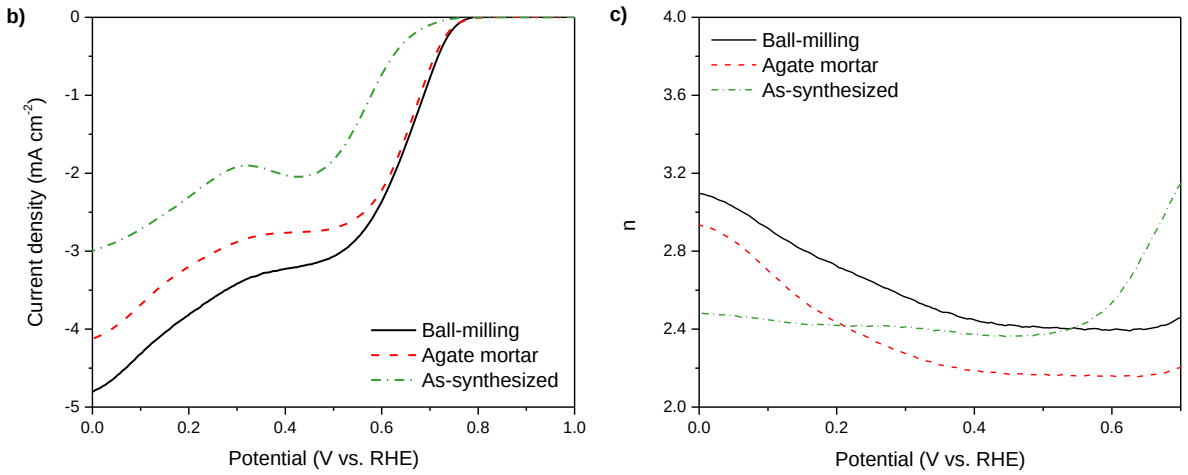

Figure 2. (a) Particle size distribution of HP-CM as-synthesized and after particle size reduction by ball milling or hand (mortar) grinding. (b) and (c): Effect of particle size on the electrochemical ORR performance of HP-CM: (b) LSV curves, and (c) number of electrons transferred, *n*, in 0.1 M KOH solution saturated with O_2 at 1600 rpm and 5 mV s^{-1}. The other conditions were: 17.9 wt.% Nafion®; carbon loading 0.25 mg cm^{-2}.

3.2.2 Electrocatalytic activity for ORR

The reduction of particle size by mortar grinding and ball milling facilitates the preparation of the carbon ink. Well-dispersed and homogeneous inks were obtained by sonication after grinding, especially for the ball-milled carbon, facilitating the deposition of a homogeneous thin layer on the glassy carbon disk, which is essential for testing the electrochemical performance for the ORR and for future application in fuel cell stations. Conversely, the as-synthesized carbon powder containing large particles led to poor ink dispersion with some flocculates even after 1 hour of sonication, and consequently to a lower quality of the carbon film in terms of coverage and homogeneity. Indeed, the surface of the disk was not fully covered by carbon particles, which led to a decrease in the effective surface of the electrode. These differences in carbon film quality led to significant deviations in the ORR performance of the materials.

Figure 2b shows the LSV curves of different RRDE electrodes drop cast with the same carbon loading and Nafion® content for HP-CM as-synthesized and after the ball or mortar grinding procedures. Table 2 summarizes the electrocatalytic results. The as-synthesized material exhibits low activity for ORR, with a similar LSV profile to that of bare glassy carbon electrode [34] due to a non-homogenous carbon film coverage. After grinding, an improved activity for oxygen reduction was found (Figure 2b), which is related to the smoother character of the catalyst film covering the entire glassy carbon electrode, thereby leading to a better electrochemical performance. Indeed, the current density increased from -2.01 mA cm^{-2} at 0.4 V vs. RHE for the as-synthesized HP-CM to -2.76 and -3.22 mA cm^{-2} for the mortar-ground and ball-milled samples, respectively (see Table 2). Additionally, a significant shift (around 70 mV) of the onset of the oxygen reduction to more positive potentials was evident after reducing the size of the carbon particles for both methods. This result is important because, unlike the results presented below, carbon grinding is the only experimental parameter studied in this work that significantly affects the E_{ONSET}, a characteristic of the kinetics for the ORR. It is also worth noting that the electron number (and hence the selectivity to hydroxide) is also substantially affected by preliminary grinding and the way in which this has been carried out (Figure 2c). The pristine HP-CM shows an electron number around 2.4 over the entire potential range, whereas after ball milling or mortar grinding, the electron number increases up to 2.9 – 3.1 at 0 V vs. RHE.

Table 2. Electrochemical data for HP-CM having different particle sizes.

Grinding	E_{ONSET} (V) at -0.1 mA·cm^{-2}	j (mA·cm^{-2}) at 0.4 V vs. RHE	j (mA·cm^{-2}) at 0 V vs. RHE	n at 0.4 V vs. RHE	n at 0 V vs. RHE
None	0.70	-2.02	-2.99	2.37	2.48
Mortar	0.75	-2.76	-4.12	2.19	2.93
Ball milling	0.77	-3.22	-4.80	2.44	3.10

In addition to the decrease in particle size and thus the homogeneous coverage of the drop-cast RRDE electrode by a smooth carbon layer, the improved activity for oxygen reduction can also be ascribed to a combined consequence of grinding-induced changes in surface chemistry, surface area or structure of the milled carbons. Milling of pristine HP-CM resulted in the generation of carbon defects and the reduction of crystallite size (see Raman spectra, Figure S5), which can positively affect the electrochemical performance for ORR, according to previous works [35–39]. On the other hand, oxygen functional groups can boost the electrocatalytic activity of carbon materials for ORR through a doping effect or hydrophilicity enhancement [35,36,40]. In addition, the presence of carbonyl groups is known to be favorable for oxygen adsorption on graphitic carbon materials, while quinones are responsible for reducing the reaction overpotential [35,41,42]. Although the influence of surface chemistry on the electrocatalytic activity for oxygen reduction of ground carbon powders cannot be completely ruled out, manual or ball milling resulted in a slight oxygen enrichment of the carbon surface, and thus the marked improvement in ORR performance cannot be explained solely by the amount or nature of oxygen functional groups. Similarly, a moderate increase in specific surface area and pore volume was observed after grinding. Nevertheless, this small texture development alone cannot explain the better kinetics of the resultant material after ball milling. However, it is difficult to separate all these effects.

In line with this statement, grinding of the commercial carbon materials C30X and CW30, already in the form of fine powders from the beginning, was carried out (Figure S7a). For these materials, ball milling resulted in a non-negligible reduction in particle size, with a main peak centred at about 10 µm, while in comparison the peak of HP-CM, a very coarse-grained material before milling, was centred at 60 µm after milling. The Raman spectra of these materials were found to be perfectly superimposable before and after grinding (Figure S7b), and therefore no structural changes have occurred. As a result, milling of the two commercial carbons did not

strongly influence the activity and selectivity for ORR, as illustrated by the LSV and electron transfer-potential curves at 1600 rpm of the two samples before and after ball milling (Figures S7c and S7d). In this case, the milling even led to a slightly negative effect, due to the corresponding slight decrease in porosity shown in Table 1.

In order to provide the best practices for the evaluation of ORR performance, we will only show the results of ball-milled HP-CM sample in the following sections, as the smaller particle size was found to be of paramount importance for obtaining a more efficient electrocatalysis for oxygen reduction.

3.3 Effect of the Nafion® content

A crucial parameter affecting the performance of electrocatalysts for the ORR is the binder content. Ionomers are usually used as binders for electrocatalysts testing in half-cells, as they facilitate the adhesion of the porous carbon material to the glassy carbon, thus preventing its detachment during RRDE (or RDE) testing at different rotation speeds. Moreover, they are useful for future application in a fuel cell, where an ionomer is essential to transport protons (or hydroxide ions in alkaline media) to the active sites. However, these polymers are not electronically conductive. Consequently, the presence of too large amounts can lead to a decrease in electrical contact between the carbon particles and between the carbon layer and the glassy carbon electrode, and thus a decrease in electrocatalytic performance for the ORR. In addition, there is always a balance to be found between the amount of binder needed and the probability that it will hinder the electrical conductivity of the working electrode.

Nafion® is the most commonly used binder in RRDE studies for ORR in both acidic and alkaline electrolytes [20,43,44]. Herein, we tested six different Nafion® weight ratios (R_{Naf}) ranging from 9.8 to 33%. R_{Naf} was defined according to Eq. (6):

$$R_{Naf}(\%) = 100 \cdot \frac{m_{Nafion}}{m_{Nafion}+m_{Carbon}} \quad (6)$$

where m_{Nafion} and m_{Carbon} are the masses of Nafion® and porous carbon deposited on the electrode disk, respectively. A constant mass of carbon from the HP-CM sample, corresponding to an areal density of 0.25 mg cm^{-2}, was used. The LSV curves and the number of electrons transferred determined by RRDE at 1600 rpm are shown in Figures 3a and 3b, respectively.

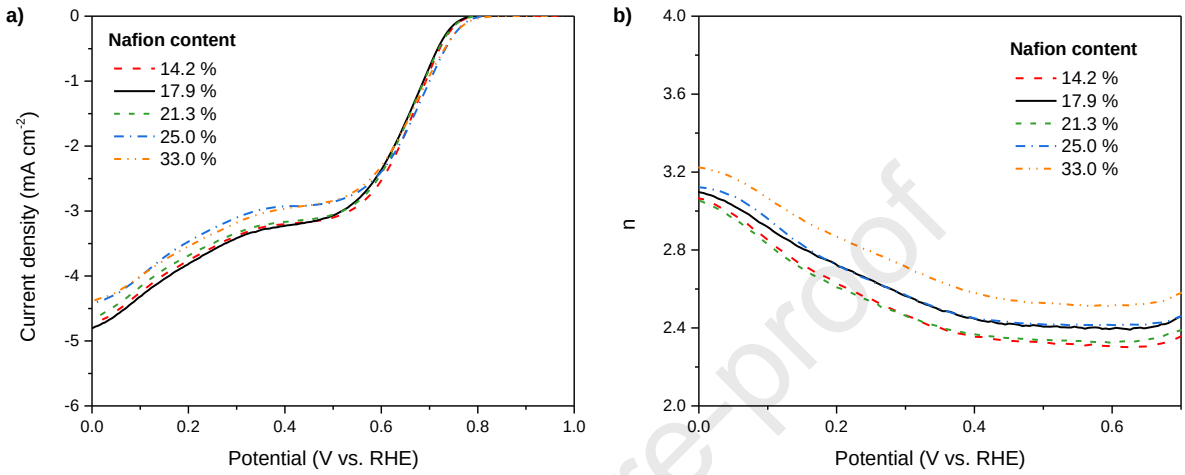

Figure 3. Effect of Nafion® loading (wt.%) on the electrochemical ORR performance of HP-CM: (a) LSV curves and (b) number of electrons transferred (*n*) in 0.1 M KOH solution saturated with O_2 at 1600 rpm and 5 mV s^{-1}. The carbon loading was 0.25 mg cm^{-2}.

A Nafion® content of 9.8 wt.% was not enough to prevent the detachment of the material, and therefore a higher ratio had to be used to obtain reproducible results. The LSV curves obtained for the three electrodes with medium loadings (14.2, 17.9 and 21.3 wt.%) are similar, suggesting that the R_{Naf} value is not critical for ORR testing in this range. However, an increase of the ratio beyond 25 wt.% led to a decrease in current density, which might be related to a partial pore blocking that leads to a higher oxygen diffusion resistance in the porosity or a higher electrical resistance along the electrode [20,43,45]. This decrease is reflected in Table 3, where the current density for ORR at 0.4 V vs. RHE shifts from -3.20 to -2.92 mA cm^{-2} for Nafion® contents of 14.2 and 33 wt.%, respectively. Additionally, a slight increase in electron number was observed with values ranging from 2.3 to 2.6 (at 0.4 V vs. RHE). This increase in electron number might be related to the longer residence time of the OOH^- intermediates as the Nafion®

content increases, which may result in a subsequent reduction within the microporosity. Other authors have obtained a similar trend for mesoporous carbon-based electrodes [20].

Table 3. Electrochemical data for Nafion ® loading experiments for HP-CM.

Nafion® content (wt.%)	E_{ONSET} (V) at -0.1 mA·cm^{-2}	j (mA·cm^{-2}) at 0.4 V vs. RHE	j (mA·cm^{-2}) at 0 V vs. RHE	n at 0.4 V vs. RHE	n at 0 V vs. RHE
14.2	0.78	-3.20	-4.76	2.35	3.06
17.9	0.77	-3.22	-4.80	2.44	3.10
21.3	0.76	-3.16	-4.66	2.36	3.05
25	0.76	-2.92	-4.44	2.44	3.12
33	0.76	-2.95	-4.42	2.58	3.24

These results show that the optimum Nafion® content for this carbon material is in the range 14 – 21 wt.%. These values are lower than those typically used in H_2-O_2 fuel-cell stations, ~ 33 wt.% for Pt/C-based electrodes. These differences indicate that the operating conditions of a fuel cell and a RRDE three-electrode system are very different. In a fuel cell, Nafion® is used as a binder but also as an ionomer that promotes proton propagation, which is not the role in the RRDE system. Moreover, while dioxygen molecules in a fuel cell station are provided by a gas flow, in RRDE measurements oxygen is provided by saturation of the working aqueous electrolyte. Finally, the cathode electrode in a fuel cell station is subjected to pressure, unlike in an RRDE test, which brings some mechanical stress. Nevertheless, the results obtained from this experimental work should not be considered as universal, since the most relevant binder content was reported to be very dependent on the nature of the carbon. Other works that have addressed this topic have indeed found much lower optimal Nafion® contents (2-8 wt.%) for a nitrogen-doped ordered mesoporous carbon with a specific surface area of about 764 m^2 g^{-1} [20]. Here, a highly porous carbon (1350 m^2 g^{-1}) was used, which could allow for greater Nafion® loading without substantial blocking of active sites.

3.4 Effect of the carbon loading

The influence on the electrochemical ORR performance of the loading of porous carbon deposited on the glassy carbon electrode was studied with the HP-CM sample. Four different carbon loadings were tested: 0.17, 0.25, 0.33 and 0.5 mg cm^{-2}, keeping R_{Naf} constant at 17.9 wt.% (see Eq. (6)).

The results of the corresponding LSV curves performed at 1600 rpm are shown in Figure 4a. The current density, expressed in mA cm^{-2}, shows that the behaviors are highly dependent on the electrode loading. The most favorable loading corresponds to 0.25 mg cm^{-2} with a current density of -3.22 mA cm^{-2} at 0.4 V vs. RHE (Table 4), followed closely by 0.33 mg cm^{-2} (-2.85 mA cm^{-2}). At the lowest carbon loading (0.17 mg cm^{-2}), the glassy carbon surface is not completely covered by HP-CM particles, and thus an enhancement of the electrochemical activity for oxygen reduction occurs as the amount of carbon increases (0.25 – 0.33 mg cm^{-2}) through a higher effective area. However, material loadings ≥ 0.5 mg cm^{-2} led to a substantial decrease in current density, from -3.22 to -0.6 mA cm^{-2} at 0.4 V vs. RHE (Table 4). This is explained by a long electron path through the electrode layer due to excessive film thickness, resulting in high electrical resistance or high mass transport resistance [21,45,46]. The latter leads to partial access to the electrochemically active sites, regardless of the intrinsic ORR activity of the material.

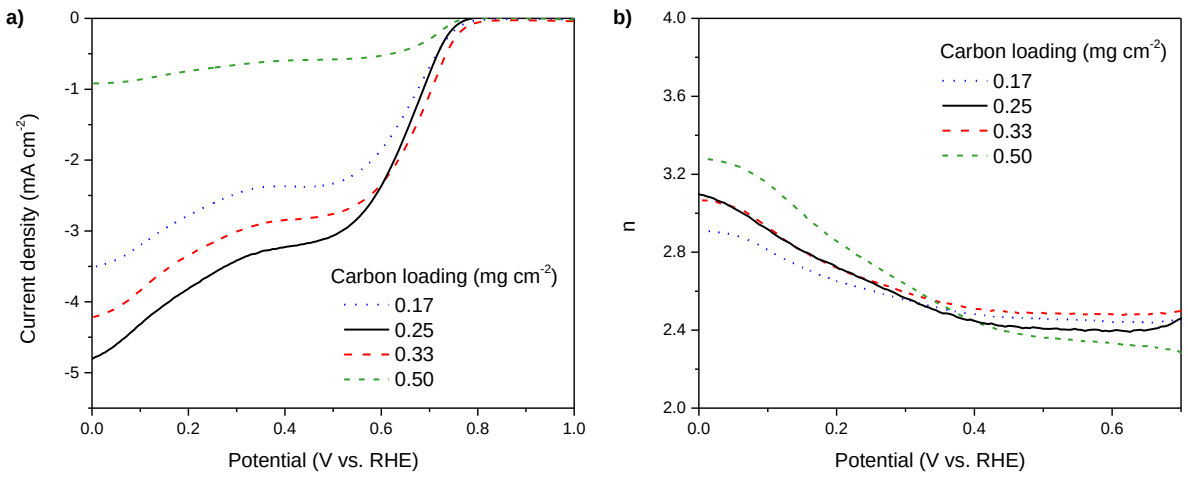

Figure 4. Effect of carbon loading on the ORR electrochemical performance of HP-CM: (a) LSV curves and (b) number of electrons transferred (*n*) in 0.1 M KOH solution saturated with O_2 at 1600 rpm and 5 mV s^{-1}. The Nafion® content was 17.9 wt.%.

This result proves that thin films are required for RRDE testing of electrocatalysts. The film thickness is directly related to the carbon loading but also to the surface area and bulk density of the materials. A wide range of loadings from 0.1 to 1.0 mg cm^{-2} has been established for different metal-free carbon electrodes by other authors [19–23]. Therefore, loading optimization is essential in order to study the electrochemical ORR performance of a new material, especially for highly porous carbon electrodes. Moreover, carbon loading seems to be a key parameter since the differences in the LSV curves are very significant compared to other factors, such as Nafion® content.

Table 4. Electrochemical data for different carbon loading for HP-CM.

Carbon loading (mg cm^{-2})	E_{ONSET} (V) at -0.1 mA·cm^{-2}	*j* (mA·cm^{-2}) at 0.4 V vs. RHE	*j* (mA·cm^{-2}) at 0 V vs. RHE	*n* at 0.4 V vs. RHE	*n* at 0 V vs. RHE
0.17	0.77	-2.37	-3.52	2.48	2.90
0.25	0.77	-3.22	-4.80	2.44	3.10
0.33	0.78	-2.85	-4.22	2.51	3.28
0.50	0.74	-0.60	-0.91	2.44	3.07

The thickness of the deposited layers appears to have an effect on the number of electrons transferred (Figure 4b), which increases with carbon loading. This makes sense since the higher the carbon loading, the higher the active area exposed to the electrolyte, which allows the ORR by-products to be retained in the carbon microporosity, and which can lead to a second reduction of OOH^- ions to hydroxide molecules via the 2-electron pathway.

3.5 Effect of the upper potential limit during ORR measurements

So far, the parameters that have been evaluated are Nafion® content, carbon loading, particle size and the importance of using an RRDE system to determine electron transfer for porous carbon materials. Another important parameter is the upper potential limit during ORR measurements, *i.e.*, the starting potential of the cathodic scan of the LSV curves in the O_2-saturated electrolyte. A sufficiently positive upper potential limit can induce electrochemical oxidation of the drop-cast carbon electrode, which has been shown to play an important role on the electrocatalytic behavior for oxygen reduction. Although the influence of electrochemical oxidation of Pt-based electrocatalysts on ORR performance has been intensively evaluated in the literature [16,47,48], a detailed study of the effect of the upper potential limit on the ORR activity and selectivity of porous carbon materials is missing. On the other hand, the ORR polarization curves of carbon-based electrocatalysts reported in the published works usually start at 1.0 V vs. RHE (cathodic direction) but different upper potential limits are also often used (from 1.0 to 1.4 V vs. RHE), which does not allow for an accurate comparison of the results.

In order to investigate the dependence of electrochemical conditioning on the activity for oxygen reduction of the HP-CM sample, eleven LSV curves were recorded using always the same lower potential limit of 0 V vs. RHE, while the upper potential limit was progressively increased from 0.88 to 1.47 V vs. RHE. Figure 5a shows a negative shift in the onset potential as the upper potential limit increases, highlighting the negative impact of electrochemical oxidation for this carbon material. A clear match between the onset potential and the starting potential is evident in Figure S8.

The improved ORR kinetics, as the upper potential limit is lower, is associated with a lower oxidation degree of the carbon surface. Carbon electro-oxidation is a complex reaction, involving the formation of various surface oxides and the complete oxidation to CO_2. This

electrochemical conditioning may introduce oxygen-containing surface groups, which can affect ORR performance. In this context, a high activity for oxygen reduction has been reported on graphitic carbons (such as carbon nanotubes or graphite) oxidized by chemical and electrochemical methods [35,36,40,49,50], although a selective production of H_2O_2 has generally been found. However, saturation of the surface by oxygen moieties may block the active sites for the ORR or hinder the diffusion of oxygen through the carbon layer, and result in lower electronic conductivity, which both decrease electrocatalytic activity [35]. In addition, non-graphitic carbon materials can undergo irreversible electrochemical oxidation to carbon dioxide (corrosion) if the upper potential limit is sufficiently high [51,52]. Nevertheless, this carbon degradation can be mitigated by a high-temperature treatment [51,52], such as that used in this work for HP-CM.

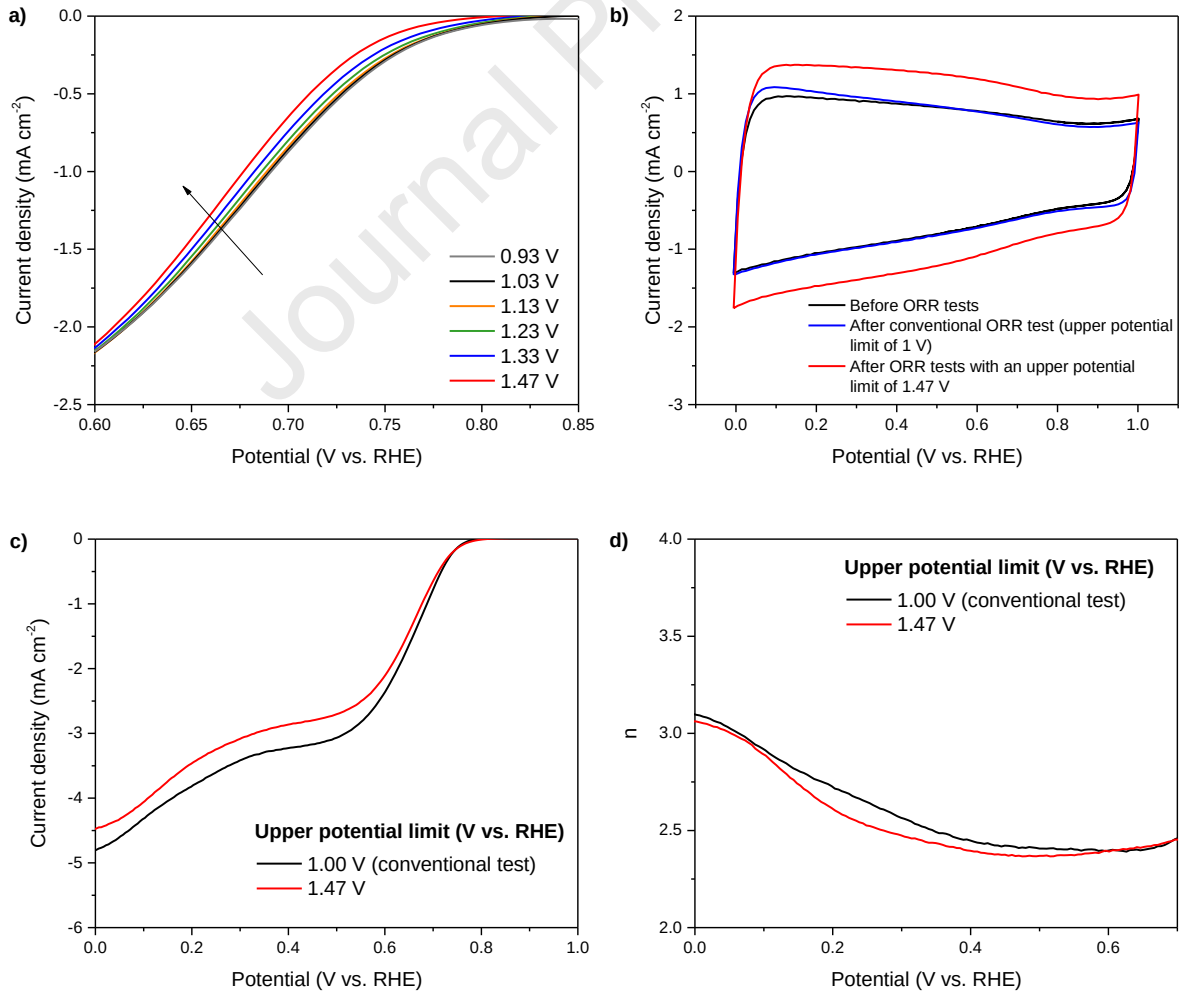

Figure 5. Effect of electrochemical conditioning on the ORR kinetics of HP-CM: (a) Zoom of LSV curves in 0.1 M KOH solution saturated with O_2 at 1600 rpm and 5 mV s^{-1}; (b) Double-layer current density vs. potential curves, at 50 mV s^{-1} in 0.1 M KOH solution saturated with N_2, for the freshly drop-cast HP-CM electrode after ORR tests using different upper potential limits; Comparison of: (c) LSV curves, and (d) number of electrons transferred, between a conventional electrochemical test (starting potential = 1 V vs. RHE) and the use of an upper potential limit of 1.47 V vs. RHE, in 0.1 M KOH solution saturated with O_2 at 1600 rpm and 5 mV s^{-1}. The other conditions were: 17.9 wt.% Nafion®, and carbon loading of 0.25 mg cm^{-2}.

To better understand the effect of electrochemical oxidation during ORR tests on the behavior of HP-CM, cyclic voltammograms were recorded at 50 mV s^{-1} in a 0.1 M KOH solution saturated with N_2. The current density-potential curves for the freshly drop-cast electrode and after ORR tests using two different upper potential limits are given in Figure 5b. A significant increase in the double-layer current was observed after ORR measurements when a starting potential of 1.47 V was used. Previous works have shown that the creation of oxygen functional groups on the carbon surface leads to higher capacitance (*i.e.*, to higher double-layer current) both through increased hydrophilicity of the carbon, the latter improving its impregnation by the electrolyte, and through pseudocapacitance contributions [51–53]. In contrast, irreversible carbon oxidation would lead to a lower double-layer current through carbonaceous material loss [51,52]. On the other hand, the capacitive behavior of HP-CM is preserved after conventional ORR testing (starting potential of 1.0 V vs. RHE). Therefore, the creation of a large extent of oxygen-containing species during the electrochemical conditioning at such positive potentials (1.47 V) seems to be the main reason for the negative shift in the onset potential for oxygen reduction. Although the generation of certain oxygen functionalities (such as carbonyl groups and quinones) on the surface of carbon materials (especially graphitic carbons) has been found to catalyze the ORR [35,41,42], the saturation of the surface by

oxygen-containing moieties may decrease the electrical conductivity [52,54], and thus decrease the electrocatalytic behavior for oxygen reduction [35]. Moreover, at such positive potentials, the electro-oxidation of carbon is expected to take place at the most reactive sites, which may be the same as those used by the ORR. This phenomenon is also observed in Pt-based electrocatalysts, in which the starting potential has a significant effect on E_{ONSET} for ORR [16]. Moreover, LSV curves for oxygen reduction showed a negative correlation between the upper potential limit and the limiting current density (Figure 5c). In a conventional test, the carbon electrode developed 3.22 mA cm^{-2} at 0.4 V vs. RHE, while a value of 2.89 mA cm^2 was obtained after electrochemical conditioning at 1.47 V vs. RHE. In addition, electrochemical oxidation resulted in a slight decrease in the number of electrons transferred, and thus a higher selectivity to produce the H_2O_2 intermediate instead of the hydroxide (Figure 5d).

Similarly, LSV at different upper potential limits of drop-cast RRDE electrodes, based on activated carbons C30X and CW30, also revealed sluggish kinetics and lower activity for oxygen reduction when the upper potential limit was increased (Figure S9 and Figure S10a). In addition, electrochemical oxidation led to a significant decrease in the number of electrons transfer, and thus to a preferential formation of H_2O_2 (Figure S10b). However, for these carbon materials, which are neither graphitic nor have been treated at high temperatures, the irreversible degradation of carbon by electro-oxidation seems to be responsible for the decrease in electrocatalytic performance, as evidenced by the partial loose of double-layer current after electrochemical conditioning at more positive potentials (Figure S11).

For comparison purposes, it would be strongly recommended to use the same potential window for all materials studied. Otherwise, an accurate discussion would not be possible. In addition, the upper potential limit must be selected to avoid irreversible oxidation of the carbon and, therefore, special attention must be given to carbonaceous materials that are non-

graphitizable or that have not been treated at high temperature. This remark applies particularly to activated carbons and in general to porous carbons derived from biomass.

4. Conclusions

In this work, the optimization of some major parameters affecting the ORR performance of porous carbon materials was considered. We have shown that:

- The RDE technique is not an accurate method to study the selectivity for oxygen reduction of porous carbon materials because the KL equation is based on flat and smooth coatings, *i.e.*, it only considers the geometric area of the electrode and not the porous surface area of the materials. Additionally, the KL method assumes that the number of electrons transferred does not depend on the rotation rate, which is not always valid. The RRDE should be always used to determine the number of electrons transferred.
- Nafion® and carbon loadings must be carefully adapted for each porous carbon, since very different optimum values can be obtained depending on the material under study. Nafion® is used as a binder in half-cells but it is an electronically non-conductive polymer. On the other hand, a high carbon loading can lead to an overly thick electrode, resulting in overshadowed catalytic performance due to a long electron path along the catalyst layer or a higher diffusion resistance through the carbon porosity.
- The upper potential limit of the cathodic scan affects the catalytic activity by electro-oxidation of the carbon material at sufficiently positive potentials. This could lead to the irreversible degradation of the carbon material by electro-oxidation or surface saturation by oxygen groups on the surface of the carbon-based electrocatalyst, which would decrease the electrical conductivity and, therefore, the activity for oxygen reduction.
- The performance of ball-milled carbons is dramatically improved compared to the non-ground carbon due to an increase in the effective electrochemical surface area of the RRDE

electrode. Moreover, the small carbon particles of homogeneous size facilitate the preparation of the ink and thus its homogenous coverage on the glassy carbon electrode.

This work thus provides important guidelines for best practices in the comparative evaluation of ORR performances and will be helpful for researchers new to the electrocatalysis of carbonaceous materials.

Acknowledgement

This study was partly supported by the French PIA project "Lorraine Université d'Excellence", reference ANR-15-IDEX-04-LUE and the TALiSMAN project funded by ERDF (2019-000214). SPR acknowledges MCIN/AEI/10.13039/501100011033 for her Juan de la Cierva Incorporación research contract (IJC2019-041874-I).

References

[1] J. Quílez-Bermejo, E. Morallón, D. Cazorla-Amorós, Metal-free heteroatom-doped carbon-based catalysts for ORR. A critical assessment about the role of heteroatoms, Carbon. (2020). https://doi.org/10.1016/j.carbon.2020.04.068.

[2] D. Liu, L. Tao, D. Yan, Y. Zou, S. Wang, Recent Advances on Non-precious Metal Porous Carbon-based Electrocatalysts for Oxygen Reduction Reaction, ChemElectroChem. 5 (2018) 1775–1785. https://doi.org/10.1002/celc.201800086.

[3] L. Du, L. Xing, G. Zhang, M. Dubois, S. Sun, Strategies for Engineering High-Performance PGM-Free Catalysts toward Oxygen Reduction and Evolution Reactions, Small Methods. 4 (2020) 2000016. https://doi.org/10.1002/smtd.202000016.

[4] V. Neburchilov, H. Wang, J.J. Martin, W. Qu, A review on air cathodes for zinc–air fuel cells, Journal of Power Sources. 195 (2010) 1271–1291. https://doi.org/10.1016/j.jpowsour.2009.08.100.

[5] C. Hu, L. Dai, Carbon-Based Metal-Free Catalysts for Electrocatalysis beyond the ORR, Angewandte Chemie International Edition. 55 (2016) 11736–11758. https://doi.org/10.1002/anie.201509982.

[6] Y. Wang, F.-L. Hu, Y. Mi, C. Yan, S. Zhao, Single-metal-atom catalysts: An emerging platform for electrocatalytic oxygen reduction, Chemical Engineering Journal. 406 (2021) 127135. https://doi.org/10.1016/j.cej.2020.127135.

[7] A. Morozan, B. Jousselme, S. Palacin, Low-platinum and platinum-free catalysts for the oxygen reduction reaction at fuel cell cathodes, Energy Environ. Sci. 4 (2011) 1238–1254. https://doi.org/10.1039/C0EE00601G.

[8] S. Pérez-Rodríguez, D. Sebastián, C. Alegre, T. Tsoncheva, N. Petrov, D. Paneva, M.J. Lázaro, Biomass waste-derived nitrogen and iron co-doped nanoporous carbons as electrocatalysts for the oxygen reduction reaction, Electrochimica Acta. 387 (2021) 138490. https://doi.org/10.1016/j.electacta.2021.138490.

[9] H. Park, S. Oh, S. Lee, S. Choi, M. Oh, Cobalt- and nitrogen-codoped porous carbon catalyst made from core–shell type hybrid metal–organic framework (ZIF-L@ZIF-67) and its efficient oxygen reduction reaction (ORR) activity, Applied Catalysis B: Environmental. 246 (2019) 322–329. https://doi.org/10.1016/j.apcatb.2019.01.083.

[10] Q. Dong, H. Wang, S. Ji, X. Wang, Q. Liu, D.J.L. Brett, V. Linkov, R. Wang, Mn Nanoparticles Encapsulated within Mesoporous Helical N-Doped Carbon Nanotubes as Highly Active Air Cathode for Zinc–Air Batteries, Advanced Sustainable Systems. 3 (2019) 1900085. https://doi.org/10.1002/adsu.201900085.

[11] L. Yang, J. Shui, L. Du, Y. Shao, J. Liu, L. Dai, Z. Hu, Carbon-Based Metal-Free ORR Electrocatalysts for Fuel Cells: Past, Present, and Future, Advanced Materials. 31 (2019) 1804799. https://doi.org/10.1002/adma.201804799.

[12] C.A. Campos-Roldán, R.G. González-Huerta, N. Alonso-Vante, Experimental Protocol for HOR and ORR in Alkaline Electrochemical Measurements, J. Electrochem. Soc. 165 (2018) J3001. https://doi.org/10.1149/2.0011815jes.

[13] Y. Garsany, O.A. Baturina, K.E. Swider-Lyons, S.S. Kocha, Experimental Methods for Quantifying the Activity of Platinum Electrocatalysts for the Oxygen Reduction Reaction, Anal. Chem. 82 (2010) 6321–6328. https://doi.org/10.1021/ac100306c.

[14] Y. Garsany, J. Ge, J. St-Pierre, R. Rocheleau, K.E. Swider-Lyons, Analytical Procedure for Accurate Comparison of Rotating Disk Electrode Results for the Oxygen Reduction Activity of Pt/C, J. Electrochem. Soc. 161 (2014) F628. https://doi.org/10.1149/2.036405jes.

[15] R. Zhou, Y. Zheng, M. Jaroniec, S.-Z. Qiao, Determination of the Electron Transfer Number for the Oxygen Reduction Reaction: From Theory to Experiment, ACS Catal. 6 (2016) 4720–4728. https://doi.org/10.1021/acscatal.6b01581.
[16] I. Katsounaros, W.B. Schneider, J.C. Meier, U. Benedikt, P.U. Biedermann, A.A. Auer, K.J.J. Mayrhofer, Hydrogen peroxide electrochemistry on platinum: towards understanding the oxygen reduction reaction mechanism, Phys. Chem. Chem. Phys. 14 (2012) 7384–7391. https://doi.org/10.1039/C2CP40616K.
[17] S. Martens, L. Asen, G. Ercolano, F. Dionigi, C. Zalitis, A. Hawkins, A. Martinez Bonastre, L. Seidl, A.C. Knoll, J. Sharman, P. Strasser, D. Jones, O. Schneider, A comparison of rotating disc electrode, floating electrode technique and membrane electrode assembly measurements for catalyst testing, Journal of Power Sources. 392 (2018) 274–284. https://doi.org/10.1016/j.jpowsour.2018.04.084.
[18] K. Shinozaki, J.W. Zack, S. Pylypenko, B.S. Pivovar, S.S. Kocha, Oxygen Reduction Reaction Measurements on Platinum Electrocatalysts Utilizing Rotating Disk Electrode Technique: II. Influence of Ink Formulation, Catalyst Layer Uniformity and Thickness, J. Electrochem. Soc. 162 (2015) F1384. https://doi.org/10.1149/2.0551512jes.
[19] A. Gabe, R. Ruiz-Rosas, C. González-Gaitán, E. Morallón, D. Cazorla-Amorós, Modeling of oxygen reduction reaction in porous carbon materials in alkaline medium. Effect of microporosity, Journal of Power Sources. 412 (2019) 451–464. https://doi.org/10.1016/j.jpowsour.2018.11.075.
[20] N. Daems, T. Breugelmans, I.F.J. Vankelecom, P.P. Pescarmona, Influence of the Composition and Preparation of the Rotating Disk Electrode on the Performance of Mesoporous Electrocatalysts in the Alkaline Oxygen Reduction Reaction, ChemElectroChem. 5 (2018) 119–128. https://doi.org/10.1002/celc.201700907.
[21] G. Zhang, Q. Wei, X. Yang, A.C. Tavares, S. Sun, RRDE experiments on noble-metal and noble-metal-free catalysts: Impact of loading on the activity and selectivity of oxygen reduction reaction in alkaline solution, Applied Catalysis B: Environmental. 206 (2017) 115–126. https://doi.org/10.1016/j.apcatb.2017.01.001.
[22] G. Zhong, S. Xu, L. Liu, C.Z. Zheng, J. Dou, F. Wang, X. Fu, W. Liao, H. Wang, Effect of Experimental Operations on the Limiting Current Density of Oxygen Reduction Reaction Evaluated by Rotating-Disk Electrode, ChemElectroChem. 7 (2020) 1107–1114. https://doi.org/10.1002/celc.201902085.
[23] E.S.F. Cardoso, G.V. Fortunato, G. Maia, Use of Rotating Ring-Disk Electrodes to Investigate Graphene Nanoribbon Loadings for the Oxygen Reduction Reaction in Alkaline Medium, ChemElectroChem. 5 (2018) 1691–1701. https://doi.org/10.1002/celc.201800331.
[24] M. Seredych, A. Szczurek, V. Fierro, A. Celzard, T.J. Bandosz, Electrochemical Reduction of Oxygen on Hydrophobic Ultramicroporous PolyHIPE Carbon, ACS Catal. 6 (2016) 5618–5628. https://doi.org/10.1021/acscatal.6b01497.
[25] J. Encalada, K. Savaram, N.A. Travlou, W. Li, Q. Li, C. Delgado-Sánchez, V. Fierro, A. Celzard, H. He, T.J. Bandosz, Combined Effect of Porosity and Surface Chemistry on the Electrochemical Reduction of Oxygen on Cellular Vitreous Carbon Foam Catalyst, ACS Catal. 7 (2017) 7466–7478. https://doi.org/10.1021/acscatal.7b01977.
[26] J. Quílez-Bermejo, E. Morallón, D. Cazorla-Amorós, Polyaniline-Derived N-Doped Ordered Mesoporous Carbon Thin Films: Efficient Catalysts towards Oxygen Reduction Reaction, Polymers. 12 (2020) 2382. https://doi.org/10.3390/polym12102382.
[27] J. Castro-Gutiérrez, A. Sanchez-Sanchez, J. Ghanbaja, N. Díez, M. Sevilla, A. Celzard, V. Fierro, Synthesis of perfectly ordered mesoporous carbons by water-assisted mechanochemical self-assembly of tannin, Green Chem. 20 (2018) 5123–5132. https://doi.org/10.1039/C8GC02295J.

[28] P. Mallet-Ladeira, P. Puech, C. Toulouse, M. Cazayous, N. Ratel-Ramond, P. Weisbecker, G.L. Vignoles, M. Monthioux, A Raman study to obtain crystallite size of carbon materials: A better alternative to the Tuinstra–Koenig law, Carbon. 80 (2014) 629–639. https://doi.org/10.1016/j.carbon.2014.09.006.
[29] Z. Jia, G. Yin, J. Zhang, 6 - Rotating Ring-Disk Electrode Method, in: W. Xing, G. Yin, J. Zhang (Eds.), Rotating Electrode Methods and Oxygen Reduction Electrocatalysts, Elsevier, Amsterdam, 2014: pp. 199–229. https://doi.org/10.1016/B978-0-444-63278-4.00006-9.
[30] G. Wu, K.L. More, C.M. Johnston, P. Zelenay, High-Performance Electrocatalysts for Oxygen Reduction Derived from Polyaniline, Iron, and Cobalt, Science. 332 (2011) 443–447. https://doi.org/10.1126/science.1200832.
[31] G. Lemes, D. Sebastián, E. Pastor, M.J. Lázaro, N-doped graphene catalysts with high nitrogen concentration for the oxygen reduction reaction, Journal of Power Sources. 438 (2019) 227036. https://doi.org/10.1016/j.jpowsour.2019.227036.
[32] A.C. Ferrari, J. Robertson, A.C. Ferrari, J. Robertson, Raman spectroscopy of amorphous, nanostructured, diamond–like carbon, and nanodiamond, Philosophical Transactions of the Royal Society of London. Series A: Mathematical, Physical and Engineering Sciences. 362 (2004) 2477–2512. https://doi.org/10.1098/rsta.2004.1452.
[33] D.B. Schuepfer, F. Badaczewski, J.M. Guerra-Castro, D.M. Hofmann, C. Heiliger, B. Smarsly, P.J. Klar, Assessing the structural properties of graphitic and non-graphitic carbons by Raman spectroscopy, Carbon. 161 (2020) 359–372. https://doi.org/10.1016/j.carbon.2019.12.094.
[34] J. Quílez-Bermejo, A. Ghisolfi, D. Grau-Marín, E. San-Fabián, E. Morallón, D. Cazorla-Amorós, Post-synthetic efficient functionalization of polyaniline with phosphorus-containing groups. Effect of phosphorus on electrochemical properties, European Polymer Journal. 119 (2019) 272–280. https://doi.org/10.1016/j.eurpolymj.2019.07.048.
[35] K.-H. Wu, D.-W. Wang, I.R. Gentle, Revisiting oxygen reduction reaction on oxidized and unzipped carbon nanotubes, Carbon. 81 (2015) 295–304. https://doi.org/10.1016/j.carbon.2014.09.060.
[36] Z. Lu, G. Chen, S. Siahrostami, Z. Chen, K. Liu, J. Xie, L. Liao, T. Wu, D. Lin, Y. Liu, T.F. Jaramillo, J.K. Nørskov, Y. Cui, High-efficiency oxygen reduction to hydrogen peroxide catalysed by oxidized carbon materials, Nature Catalysis. 1 (2018) 156–162. https://doi.org/10.1038/s41929-017-0017-x.
[37] G. Zhong, H. Wang, H. Yu, H. Wang, F. Peng, Chemically drilling carbon nanotubes for electrocatalytic oxygen reduction reaction, Electrochimica Acta. 190 (2016) 49–56. https://doi.org/10.1016/j.electacta.2015.12.216.
[38] G. Zhong, H. Wang, H. Yu, F. Peng, The effect of edge carbon of carbon nanotubes on the electrocatalytic performance of oxygen reduction reaction, Electrochemistry Communications. 40 (2014) 5–8. https://doi.org/10.1016/j.elecom.2013.12.017.
[39] C. Greco, U. Cosentino, D. Pitea, G. Moro, S. Santangelo, S. Patanè, M. D'Arienzo, M. Fiore, F. Morazzoni, R. Ruffo, Role of the carbon defects in the catalytic oxygen reduction by graphite nanoparticles: a spectromagnetic, electrochemical and computational integrated approach, Phys. Chem. Chem. Phys. 21 (2019) 6021–6032. https://doi.org/10.1039/C8CP07023G.
[40] X. Wang, C. Ouyang, S. Dou, D. Liu, S. Wang, Oxidized carbon nanotubes as an efficient metal-free electrocatalyst for the oxygen reduction reaction, RSC Adv. 5 (2015) 41901–41904. https://doi.org/10.1039/C5RA05172J.
[41] E. Yeager, Electrocatalysts for O2 reduction, Electrochimica Acta. 29 (1984) 1527–1537. https://doi.org/10.1016/0013-4686(84)85006-9.

[42] A. Sarapuu, K. Helstein, K. Vaik, D.J. Schiffrin, K. Tammeveski, Electrocatalysis of oxygen reduction by quinones adsorbed on highly oriented pyrolytic graphite electrodes, Electrochimica Acta. 55 (2010) 6376–6382. https://doi.org/10.1016/j.electacta.2010.06.055.
[43] M. Roca-Ayats, M.D. Roca-Moreno, M.V. Martínez-Huerta, Optimization of alkaline catalytic inks for three-electrode electrochemical half-cell measurements, International Journal of Hydrogen Energy. 41 (2016) 19656–19663. https://doi.org/10.1016/j.ijhydene.2016.06.168.
[44] J. Quílez-Bermejo, K. Strutyński, M. Melle-Franco, E. Morallón, D. Cazorla-Amorós, On the Origin of the Effect of pH in Oxygen Reduction Reaction for Nondoped and Edge-Type Quaternary N-Doped Metal-Free Carbon-Based Catalysts, ACS Appl. Mater. Interfaces. 12 (2020) 54815–54823. https://doi.org/10.1021/acsami.0c17249.
[45] U.A. Paulus, T.J. Schmidt, H.A. Gasteiger, R.J. Behm, Oxygen reduction on a high-surface area Pt/Vulcan carbon catalyst: a thin-film rotating ring-disk electrode study, Journal of Electroanalytical Chemistry. 495 (2001) 134–145. https://doi.org/10.1016/S0022-0728(00)00407-1.
[46] D. Shin, B. Jeong, M. Choun, J.D. Ocon, J. Lee, Diagnosis of the measurement inconsistencies of carbon-based electrocatalysts for the oxygen reduction reaction in alkaline media, RSC Adv. 5 (2014) 1571–1580. https://doi.org/10.1039/C4RA12209G.
[47] K.J.J. Mayrhofer, G.K.H. Wiberg, M. Arenz, Impact of Glass Corrosion on the Electrocatalysis on Pt Electrodes in Alkaline Electrolyte, J. Electrochem. Soc. 155 (2007) P1. https://doi.org/10.1149/1.2800752.
[48] A. Kongkanand, J.M. Ziegelbauer, Surface Platinum Electrooxidation in the Presence of Oxygen, J. Phys. Chem. C. 116 (2012) 3684–3693. https://doi.org/10.1021/jp211490a.
[49] A.B. Soliman, H.S. Abdel-Samad, S.S. Abdel Rehim, H.H. Hassan, Surface functionality and electrochemical investigations of a graphitic electrode as a candidate for alkaline energy conversion and storage devices, Scientific Reports. 6 (2016) 22056. https://doi.org/10.1038/srep22056.
[50] C. Paliteiro, A. Hamnett, J.B. Goodenough, The electroreduction of oxygen on pyrolytic graphite, Journal of Electroanalytical Chemistry and Interfacial Electrochemistry. 233 (1987) 147–159. https://doi.org/10.1016/0022-0728(87)85012-X.
[51] S. Pérez-Rodríguez, D. Sebastián, M.J. Lázaro, Insights on the Electrochemical Oxidation of Ordered Mesoporous Carbons, J. Electrochem. Soc. 167 (2020) 024511. https://doi.org/10.1149/1945-7111/ab6a8f.
[52] S. Pérez-Rodríguez, D. Sebastián, M.J. Lázaro, Electrochemical oxidation of ordered mesoporous carbons and the influence of graphitization, Electrochimica Acta. 303 (2019) 167–175. https://doi.org/10.1016/j.electacta.2019.02.065.
[53] S. Pérez-Rodríguez, E. Pastor, M.J. Lázaro, Electrochemical behavior of the carbon black Vulcan XC-72R: Influence of the surface chemistry, International Journal of Hydrogen Energy. 43 (2018) 7911–7922. https://doi.org/10.1016/j.ijhydene.2018.03.040.
[54] S. Pérez-Rodríguez, D. Torres, M.J. Lázaro, Effect of oxygen and structural properties on the electrical conductivity of powders of nanostructured carbon materials, Powder Technology. 340 (2018) 380–388. https://doi.org/10.1016/j.powtec.2018.09.038.

Declaration of interests

☒ The authors declare that they have no known competing financial interests or personal relationships that could have appeared to influence the work reported in this paper.

☐The authors declare the following financial interests/personal relationships which may be considered as potential competing interests: